Progress in Propulsion Physics **4** (2013) 113-132
DOI: 10.1051/eucass/201304113

LARGE EDDY SIMULATIONS AND EXPERIMENTS OF NONLINEAR FLOW INTERACTIONS IN HYBRID ROCKET COMBUSTION

Y. Na[1] and C. Lee[2]

[1]Department of Mechanical Engineering, Konkuk University
Seoul 143-701, Korea

[2]Department of Aerospace Engineering, Konkuk University
Seoul 143-701, Korea

Nonlinear combustion phenomenon was investigated through an experiment in a hybrid rocket motor. A poly(methyl methacrylate) (PMMA) / gaseous oxygen (GOx) combination was used with several types of disks equipped in a prechamber with the aim of modifying the local turbulent flow. By allowing this disturbance generated in a prechamber to interact with the shedding vortex inherently produced in the main chamber, a possibility of commonly observed nonlinear combustion feature such as DC-shift was analyzed. In a baseline test, a vortex shedding occurs due to the interaction of a main oxidizer flow with the evaporated fuel stream coming out of the surface during the regression process. Among the several types of disks, it turned out that only the disk4 produced the excitation which subsequently suppressed the vortex shedding phenomenon in the main chamber. This descent interaction was reflected in a sudden pressure drop (which may be described as direct current (DC) shift) of about 10 psi in the time history of the pressure during the nominal combustion. The present result with the disk4 suggests the possibility of phase cancellation between the excitation induced by the disk4 and the shedding vortex but much more work should be conducted to extract more accurate correlation of the phase information. In order to understand the baseline flow physics, a compressible large eddy simulation (LES) was conducted with the prescribed wall blowing boundary condition. The result clearly exhibited the existence of vortex shedding phenomenon with a specified frequency. The fact that important flow features of the present computation are quite similar to those obtained with an incompressible assumption in a flat channel suggests that both compressibility and curvature effects do not dominate in the present flow configuration.

1 INTRODUCTION

Hybrid rocket is attracting much attention recently because of its excellent safety features, relatively high performance compared to solid rocket motor, thrust control capability, and low development cost. However, the density specific impulses lower than the one for the solid rocket motor is the major drawback in applying to the practical propulsive systems. Much effort is currently being made towards enhancing the regression rate of a hybrid fuel. Even though various efforts have been attempted to understand the flow physics in the past, significant improvement of regression rate is likely to be made only after gaining a better understanding of the flow instability associated with a flow interaction between a main oxidizer flow and evaporated fuel flow.

Lee and Na [1–3] visualized the sequential changes of near-surface flow patterns during PMMA combustion. Visualization shows that flow started with a streaky pattern of coherent vortices elongated in the axial direction at the initial stage of combustion. This is the typical features of conventional turbulent flow structure. And the flow interactions with evaporated fuel flow produce the sudden change of visualized features from a streaky to an isolated cell pattern by modifying the boundary layer structures.

Also, LES studies by Lee and Na [2, 3] were conducted for a transpired channel to investigate the effect of wall blowing on the modification of turbulence structure without accounting for chemical reactions. Basically, flow dynamics in solid rocket motor is different from the internal flow in hybrid rocket combustion where the oxidizer is introduced into the chamber as a fully developed turbulent flow and then subsequently interacts with the surface injection. As seen in the case of solid rocket combustion, their results showed a flow oscillation with a specific dominant frequency near the surface. This flow oscillation was attributed to the result of the interaction between an oxidizer stream and an evaporating fuel flow from the surface. This oscillation is quite analogous to the flow pattern observed in a long solid rocket motor, known as parietal vortex shedding. In this aspect, it is not surprising to expect that the hydrodynamic instabilities observed in the solid propellant combustion could be possibly developed in hybrid rocket as well.

During the interaction of the oxidizer stream with the vertical momentum generated by the regression process, shear instability resulting from the intensive mixing develops and a distinct time-scale is imposed to the flow in the subsequent development of the flow. Occurrence of the large time-scale in the flow field indicates, perhaps, that the flow is dominated by the Kelvin–Helmholtz type instability. Also, the combustion process is expected to be directly influenced by the formation of the time-scale of the specific frequency in the turbulent flow. Since the range of length-scale (or, equivalently, time-scale) of the combustion process is different from that of the background turbulent flow, it is not easy to directly identify the effect of flow instability on the combustion but such an effort will be a very meaningful attempt for the understanding of the flow physics in the hybrid rocket motor.

An abrupt increase in pressure during combustion, known as DC-shift, is one of the typical examples of nonlinear phenomena usually observed in solid propellant combustion. And the term of "DC-shift" refers to the sudden rise of measured voltage corresponding to chamber pressure. Even though the triggering mechanism of DC-shift is not completely understood yet, experimental data showed that DC-shift is likely to occur when burning rate increases in the presence of internal gas oscillations parallel to propellant surface.

Many researches have been done to identify the main mechanism of DC-shift during the combustion. Malhotra and Flandro [4] are one of the pioneers who proposed a model for understanding the origin of DC-shift. In irrotational flow fields, the vorticity is created in the vicinity of propellant surface by the interaction between acoustic waves with mean flow field. The pressure gradient existing in the combustion chamber can be the source of the flow turning or vorticity formation if this interacts with an incoming flux of evaporated propellant flow normal to the surface. This phenomenon is easily understood by means of Crocco's theorem.

Flandro *et al.* [5] also have demonstrated a predictive algorithm for DC-shift based on the comprehensive nonlinear combustion instability models. Their analysis includes very complicated nonlinear models such as steep-fronted, shock pressure waves, effects of irrotational flow interactions, combustion coupling effects, and pressure coupling with the oscillatory flow field. Especially, the role of steep-fronted waves was particularly emphasized in their demonstration. The results showed a quite good agreement in predicting the evolution of the oscillation amplitude and the mean pressure shift.

Several tests with hybrid rocket motor have also reported a nonlinear behavior of combustion showing a sudden increase in combustion pressure and regression rate [6–8]. Avres and Jones [7, 8] proposed several scenarios for the initiation of DC-shift including

(i) sudden increase of throat area;

(ii) abrupt increase in propellant mass flow rate; and

(iii) sudden increase in the characteristic velocity C^*.

Note that throat area (A^*) increases gradually if it was not protected properly during the combustion. And the mass flow rate can be generally controlled. Thus, scenario of (i) and (ii) may be ruled out from the possible triggering mechanisms of DC-shift. They concluded the instantaneous increase in C^* is a plausible candidate for DC-shift. The most interesting finding, however, is that a sudden pressure drop (called a negative DC-shift) was observed as well in some test conditions, which has been never reported in solid propellant combustion.

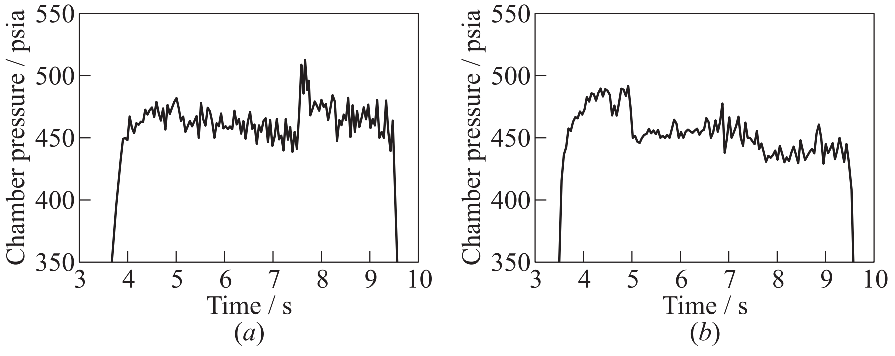

Figure 1 Positive (a) and negative (b) DC-shift observed in the experiments [7]

Figure 1 is the comparison of negative and positive DC-shifts of combustion pressure measured in the hybrid rocket combustion with hydroxyl-terminated polybutadiene (HTPB) / liquid oxygen (LOx).

A series of ramjet tests with air and PMMA by Dijkstra [6] also reported a sudden increase of pressure. Test configuration was very similar to the one used in the test for DC-shift of hybrid rocket combustion in that it installed a diaphragm at the front end of fuel grain. The regression rate was measured using an ultrasonic device. The results showed that the initiation of DC-shift coincided with the time when the regression rate suddenly increased. This implies that DC-shift is the result of the sudden increase in regression rate of solid propellant.

Tests with 11-inch hybrid rocket motor were also conducted by Boardmann *et al.* [9] and provided very interesting features of combustion oscillations including DC-shift. They used HTPB/polycyclopentadiene (PCPD) solid fuel with LOx injection. Each test was designed to investigate the effect of different test conditions combined with different prechamber geometry, injection configurations, bluff-body flame holders, and fuel inhibitors on the combustion behavior. The test results showed that the initiation of DC-shift is not associated with nozzle and flow rate conditions but with the modification of flow condition by vortex shedding. The flow field developed by the injector types and prechamber configuration was found to play a dominant role in determining the characteristics of combustion instability.

Recently, Carmicino [10] performed combustion tests with two different injector configurations: axial and radial injectors. The results showed the characteristics of combustion stability were strongly dependent upon the injector configuration. Also, they found that the axial injector did not induce either any combustion instabilities or nonlinear behavior because the longitudinal acoustic perturbations could be easily damped out. However, the radial injector could induce vortex shedding in the prechamber and generate the periodic unsteady heat release. Even with their findings that the interaction of periodic unsteady heat release with acoustic oscillations through vortex shedding had the triggering mechanism of DC-shift, they did not explain why negative DC-shifts were still observed in the test with certain flow conditions in terms of vortex shedding and oscillatory flow near the surface.

Reviewed with experimental observations in solid and hybrid rocket combustion, it can be summarized that DC-shift is the result of the sudden increase in the regression rate due to an enhanced heat transfer to the propellant caused by the oscillatory gas motion associated with vorticity formation. In spite of the physical validity of the triggering mechanism of DC-shift, the mechanism seems only to be available to validate the positive DC-shift. Since the oscillatory gas motion near the surface can rather dramatically increase the convective heat transfer, a negative DC-shift possibly associated with the reduction of heat transfer cannot be explained by the existence of oscillatory gas motion on the surface. Thus, a new scenario applicable to both positive and negative DC-shift in hybrid rocket combustion is required. And this is the main objective of the present study.

Motivated by the necessity of a new scenario, this study put some emphasis on the analysis of the occurrence of specific time-scale of surface flow oscillation resulting from the flow instability and the evolution of DC-shift linked with vortex shedding in hybrid rocket combustion. Thus, combustion tests with a PMMA/GOx were conducted with different disks located in the prechamber to investigate the effect of resonance between flow perturbation and an unsteady heat release on the nonlinear combustion. Also, compressible LES was conducted for a flow in a circular duct configuration with an imposed wall blowing at the Reynolds number which is comparable to that of the experiment. Since a circular duct better represents the real combustion geometry for the measurement tests, LES result is expected to better predict the flow patterns and oscillatory motions near the surface.

2 NONLINEAR CHARACTERISTICS OF HYBRID ROCKET COMBUSTION

A schematic of the experimental setup for the combustion test is shown in Fig. 2. Main body consists of pre-, main, and postchambers. Both pre- and postchambers had the dimension of 50 mm in diameter and 50 mm in length. The extent of the main chamber was set to 200 mm. As the combustion went on, the regression process produced the evaporated stream out of the surface. Therefore, it is expected to have a very strong shear layer developing away from the wall due to an intensive mixing between the main oxidizer flow and the evaporated stream emanating from the fuel surface.

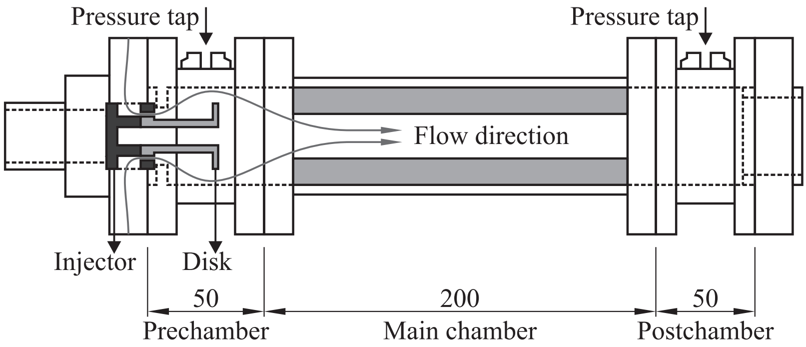

Figure 2 Schematic of the experimental setup for combustion test. Dimensions are in millimeters

To investigate the effect of flow modification on the nonlinear combustion process, several types of disturbances can be imposed to the baseline flow configuration. One of the commonly adopted methodologies is to modify the injector geometry so that the local flow in the prechamber is disturbed in a controlled way. There are several studies in the literature on this issue but, particularly, Carmicino [10] reported very interesting fact that different types of injector configuration could totally change the subsequent combustion process. More specifically, the pressure spectra obtained with a radial type injector showed an indication of quite unstable combustion as seen in a DC-shift phenomenon.

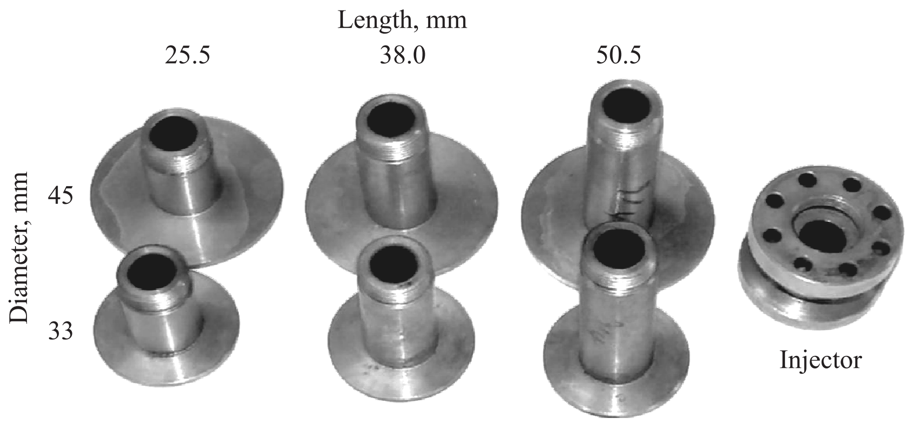

Figure 3 Axial injector and six different disks used to produce shedding vortices in the prechamber

However, any axial type injector did not lead to an unstable combustion. Obviously, a sudden pressure change indicating an unstable combustion resulted from the modification of the baseline flow. Since there is a strong coupling present between the flow dynamics and the combustion process, the reason for this abrupt change cannot be identified easily. It is just conjectured that the disturbance introduced by a radial type injector (such as additional vortex occurring in the prechamber) triggered the nonlinear combustion behavior in the main chamber [10].

With the aim of producing various kinds of excitations in the prechamber, several types of disks with different dimensions were chosen: the 1st family of the disk with a diameter of 33 mm and the 2nd family of the disk with a diameter of 45 mm. Thus, six different types of disks (shown in Fig. 3) were equipped at

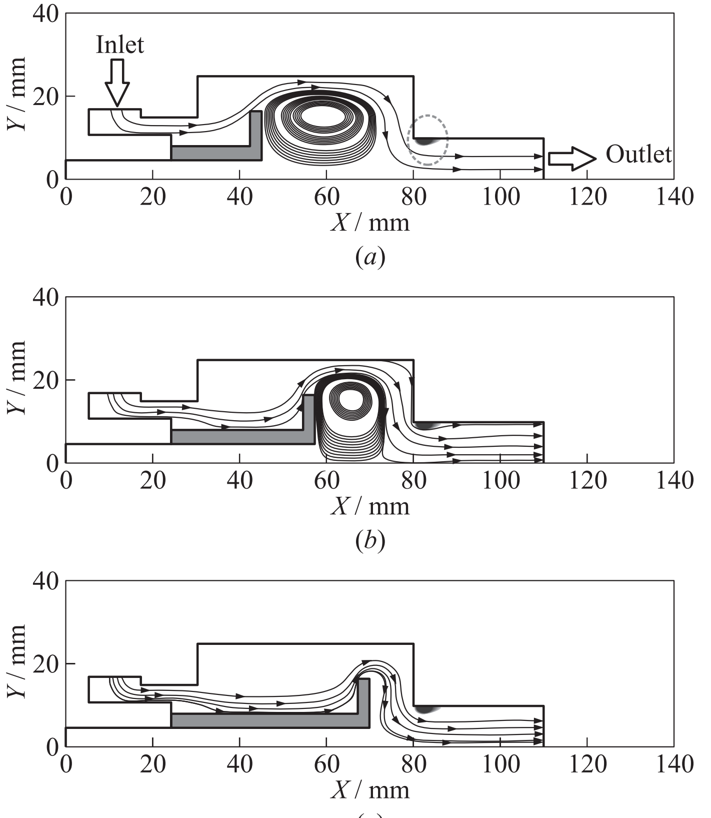

Figure 4 Schematic of prechamber with different disk locations: (*a*) 25.5 mm; (*b*) 38.0; and (*c*) 50.5 mm

three different positions (12.5, 25.0, and 37.5 mm downstream from the injector plane, respectively).

For convenience, a popular combination of PMMA/GOx was used. For the control of the oxidizer flow rate, PLC (Programming Logic Controller) and solenoid valve were used to produce the flow rate ranging from 10 to 30 g/s. The pressure information obtained with pressure gages (PMP4070) were processed using Labview software. Also, after the test, cut view of the main chamber was investigated visually to check if any peculiar flow patterns had developed.

Figure 4 shows the overall flow features associated with the configurations with different types of disks used in the present study. Dependent on the locations of the disk in the prechamber, the flows exhibit quite different kinematics. Induced flow pattern in this way, in turn, is likely to influence on the subsequent evolution of the flow in the main chamber. As stated earlier, the shedding vortex generated through the mixing process of the oxidizer flow with the evaporated gas from the fuel surface is one of the important features in the main chamber. Therefore, the interaction of the vortical structures formed in the prechamber with those inherently present in the main chamber is subject to main investigation of the present experiment.

Characteristics of Combustion Pressure

The state of combustion can be monitored by detecting the pressure fluctuations in the main chamber. Since the existence of any nonlinear combustion usually appears in the form of sudden jump or depreciation of pressure, baseline test without any disk was investigated first.

Figure 5 shows the time history of chamber pressure in both physical and frequency domains. In the frequency domain, three specially-excited regions (denoted by I, II, and III, respectively) were found. The first region I of those extra excitations was detected in the frequency range of 480–520 Hz. Since this signal appeared in the early stage of the combustion and lasted only for about 4 s before the chamber pressure approached a steady value, it is thought that the initial transient of the combustion process was detected in this time period. Initial transient should include a vortical structure formed in the region of contraction at the end of prechamber as shown in Fig. 4. As the combustion proceeds, this sharp corner is likely to be faded out and the excitation noted in the pressure signal in this frequency range is expected to die out. After the initial transients, region II was followed starting from $t = 8$ s. This region is characterized by the frequency range of 520–640 Hz. The reason for the appearance of this region is not clearly understood but it is thought to be induced by the presence of postchamber.

As shown in Fig. 2, the postchamber attached to the main chamber tends to generate spanwise vortices and the time characteristics of those vortical struc-

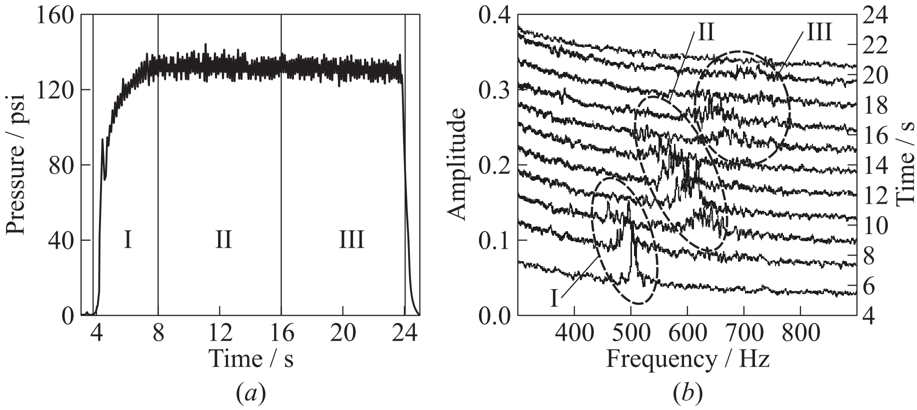

Figure 5 Combustion chamber pressure trajectory and frequency waterfall of baseline test: (*a*) combustion pressure; and (*b*) frequency waterfall

tures are likely to be reflected in the pressure signal. In fact, the frequency value predicted by using the method described in [10] was found to be approximately 600 Hz and, thus, it is believed that the region *II* shows the effect of postchamber on the flow field.

Finally, the region *III* in Fig. 5 located in the range of 650–700 Hz started from $t = 16$ s and lasted until the end of the test. The amplitude in this region is relatively smaller compared to those of regions *I* and *II*. The reason for the appearance of the region *III* is not clear at the moment and a more careful investigation is required. The decreased flow rate of the oxidizer should have changed the flow characteristics and pressure but the pressure measurement alone in the current study was not able to reveal the proper explanation.

Figure 6 shows the pressure–time history for the case with disk4. For this test case, a pressure drop of 10 psi was found during the combustion process. To check the repeatability of the experiment, three different realizations were displayed together in Fig. 6. Therefore, it appears that this rather peculiar behavior is physically realistic. The magnitude of the pressure depreciation is not large but this phenomenon is reminiscent of the negative DC-shift reported in literature [8]. Relatively small amount of pressure drop is presumably attributed to relatively smaller regression rate resulting from the use of PMMA. In general, the material of HTPB grain typically used in literature is known to easily burn compared to the popular PMMA grain. In the relatively soft fuel such as HTPB, a higher regression rate can be obtained and, as a result, a bigger pressure change (either increase or drop) will be expected in the case of unstable combustion.

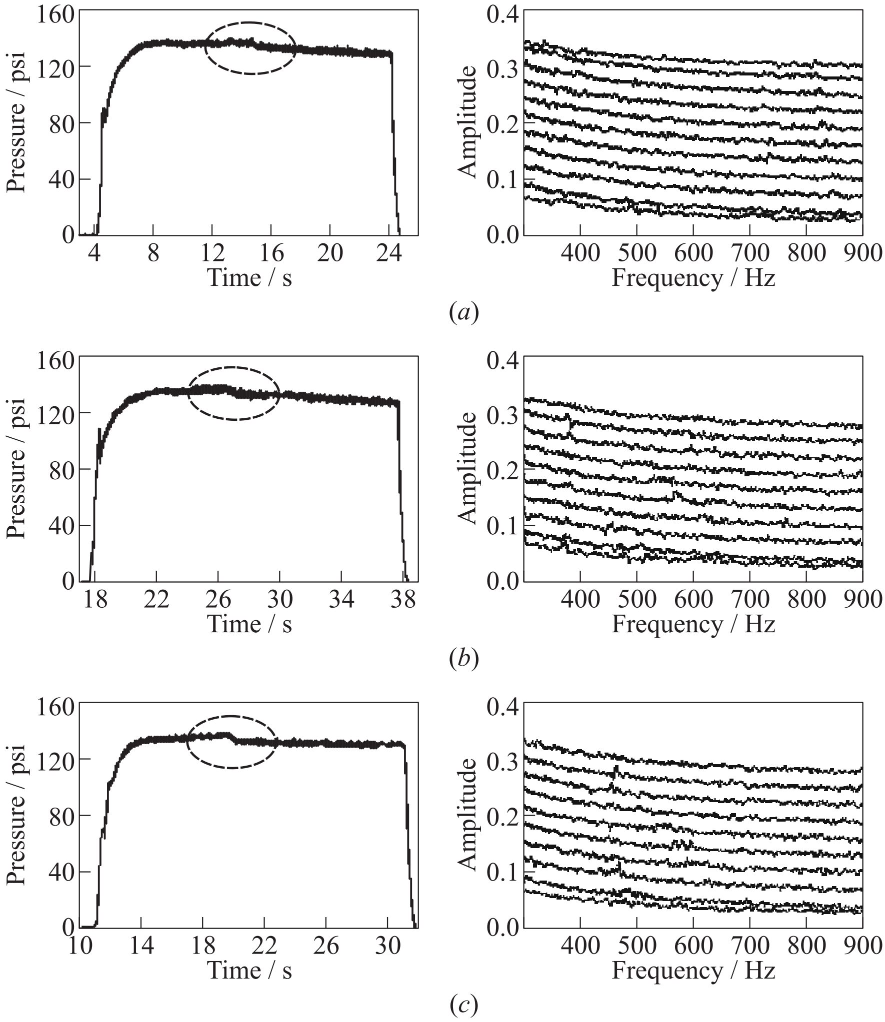

Figure 6 Repeatability of pressure drop observed from three tests with disk4

It turned out that the tests with disk2 and disk5 yielded very similar combustion characteristics. Any trace of unstable combustion was not detected and thus, the pressure signals were found to be very similar to those of the baseline test. Also, disk3 and disk6 exhibited the qualitatively similar behavior. Since the disk was placed very close to the entrance of the main fuel grain in these test cases, strong vortices were not formed in the prechamber and, thus, the region influenced by the initial transient such as region *I* shown in Fig. 5 was not detected.

The pressure signal shown in Fig. 6 suggests that the excitation produced in the prechamber acted to discourage the combustion. The link of flow information between the pre- and main chambers is not clearly understood but it is likely that the shedding vortices inherently present in the main chamber were suppressed in this situation. If this is the case, the missing information in the present analysis will be the phase correlation. That is, exact phase information of the pressure should be provided to check if the excitation produced in the prechamber would raise or suppress the shedding vortices in the main chamber.

Recent LES studies by Lee and Na [1–3] and Kim *et al.* [11] showed a very interesting feature of interaction of an oxidizer axial flow and vertical fuel flow evaporated from the surface in a flat-channel flow. They reported the existence of shedding vortices in the main chamber but the compressibility and curvature effects were not included. Therefore, numerical simulation about the baseline test was attempted in the present study to explore the compressibility effect and to provide the detailed flow field information. This issue is discussed in the next section.

In Fig. 7, cross-sectional view of the fuel grain after the combustion test was shown. As stated earlier, the test case with disk4 yielded a sudden pressure drop during the combustion test. Therefore, the flow features for the case 4 is expected to be quite different and it was hoped that Fig. 7 revealed the clue

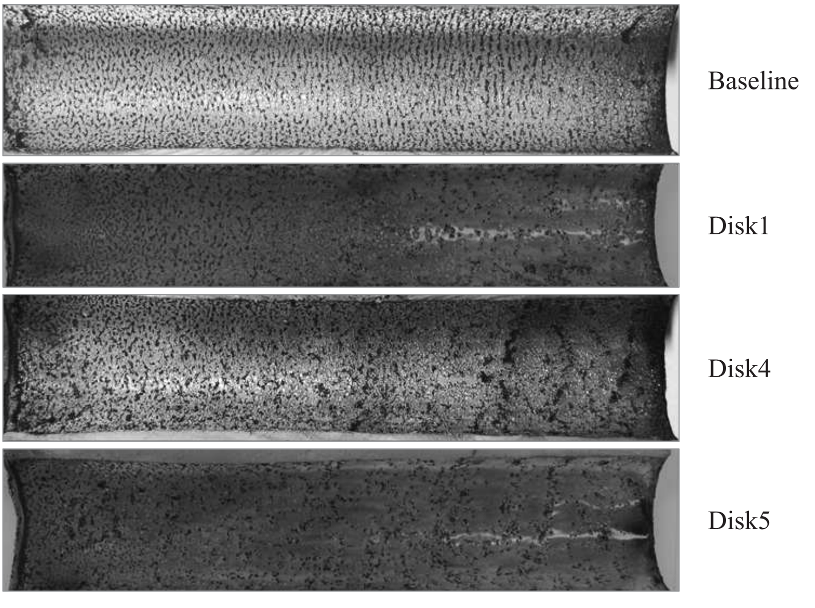

Figure 7 Cut views of fuel grain after combustion test

for the negative DC-shift like phenomenon. The test case with disk4 shows the hint that the spiral motion existed in the second half of the chamber. Unfortunately, it is not clear if this peculiar shape resulted from the characteristics of excitation produced in the prechamber. This issue will be further pursued in the future.

3 LARGE EDDY SIMULATION OF A CYLINDRICAL DUCT FLOW WITH WALL BLOWING

As was noted in the accompanying combustion test, the regression process plays an important role in the evolution of turbulent structures. The gasification process near the surface is very complicated and difficult to understand but the overall effect of this regression process can reasonably be represented by the added momentum in the vertical direction from the surface. Therefore, this wall-blowing stream interacts with the main oxidizer flow to produce a strong shear layer slightly away from the wall. Subsequently, this mixing layer with a high shear becomes unstable from fluid mechanics point of view and this is the region where the large-scale vortices with a large magnitude of spanwise vorticity are generated. These large-scale motions produce several notable features. First, this quasi-periodic motion is characterized by a high magnitude spanwise vorticity. As noted in early studies [3, 11], a specific time characteristics (or specific Strouhal number) were imposed on this motion. Interaction of this large-scale motion with quasi-streamwise vortices near the surface is expected to modify the near-wall turbulence mechanics significantly and, in turn, it affects the regression process.

Understanding of this modified flow in the vicinity of the wall is likely to be very important for the stable operation of the hybrid rocket. In order to understand many flow features found from the experimental observation, a numerical simulation was attempted in an idealized geometry as shown in Fig. 8. In a conceptual diagram of a hybrid rocket, an oxidizer is supplied to the fuel grain. This rocket motor was idealized by a circular combustion chamber without a prechamber. For simplicity, any equipment such as disk which was introduced in the accompanying experiment was not used here. Thus, a main attention was given to the interaction of the oxidizer flow with the blowing stream supplied at the surface. Also, a cold flow without combustion was considered so that variations of density and temperature were not included here.

The earlier studies for the flow in a flat channel with an incompressible assumption [2] showed that large-scale structures were characterized by Strouhal number of about 8.5. Existence of this particular time-scale suggested that Kelvin–Helmholtz type instability developed in the mixing layer and, as a result, quite large roller-like structures were shed at the specified frequency. In addition

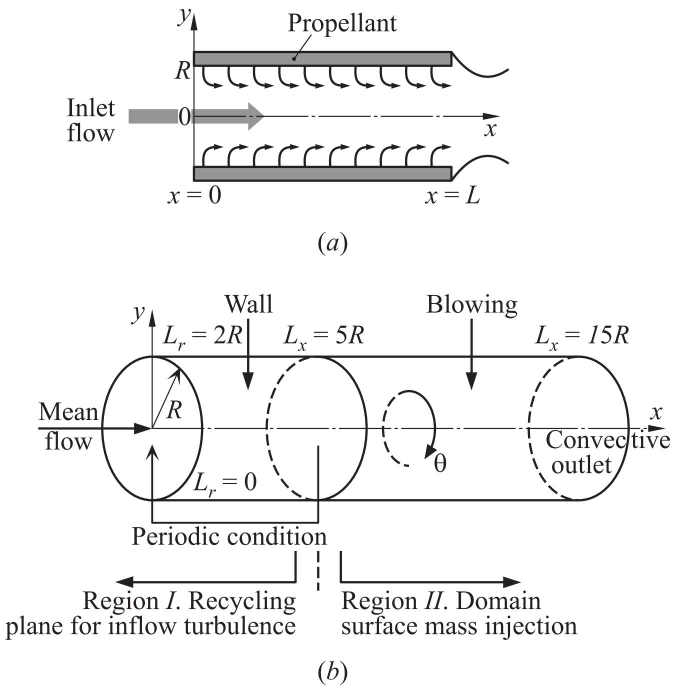

Figure 8 Computational domain for a cylindrical duct: (*a*) conceptual diagram; and (*b*) idealized computational domain of fuel port

to this presence of large-scale structures, kinematics of quasi-streamwise structures was found to be modified due to the vertical momentum applied at the surface. It was also shown that isolated cell-like patterns left behind the combustion test found on the fuel surface (as shown in Fig. 7) have to do with this kinematic modification of near-wall structures. One of the limitations of those previous works comes from the assumption of incompressible flow and from the absence of curvature effect of the circular duct. It is widely known that the curvature does not have significant effect of the near-wall turbulence mechanics if the radius of curvature is not too small. Also, the Reynolds number considered in those studies did not represent the supersonic range and, thus, it is expected that effects of both curvature and compressibility do not change the flow features found in previous works. To validate this presupposition, an LES in a cylindrical geometry was conducted to better represent large-scale structures developed in the present geometry. This simulation is expected to predict the more realistic physics on the evolution of turbulence and the characteristics of oscillatory flow in the vicinity of wall due to the direct geometric similarity with the experimental tests. The present LES is based on a compressible flow on a structured grid system. The MPI (Message Passing Interface) technique was adopted to take into account the parallel computations. The details of numerical methodology can be found in [11].

Figure 8 shows how the three-dimensional (3D) computational domain for the present study was simplified. The streamwise extent of the domain was set to $L_x = 15R$ and the spanwise extent to $L_z = 2R$ where R is the radius of a duct. The Reynolds number was set to match that of the experiment test. Since an unsteady computation requires continuous feeding of physically realistic to the main region of interest with a wall injection and, thus, a simple recycling duct (without wall injection) of length of about $5R$ was placed in front of the main region for the generation of inflow turbulence. It turned out that the length of $5R$ was long enough to produce realistic turbulence. The numerical details for the analysis are similar to [11].

In region I of Fig. 8*b*, no-slip boundary condition was assumed along the surface (i. e., $x < 5R$) but the vertical mass injection simulating a regression process was applied in region II. The injection velocity was prescribed to vary linearly from 0% to 3% of the centerline velocity of the bulk flow at the inlet of region II. Since region I was placed for the purpose of generating the unsteady turbulent inflow condition with wall injection, the effect of vertical momentum prescribed at the surface can only be found in region II. However, by directly comparing the results between regions I and II, one can isolate the effect of wall blowing quite conveniently. At the exit of region II, the convective boundary condition was used in order to allow the smooth propagation of turbulent structures with minimum interaction with the exit boundary. In fact, this boundary condition was found to work only for the relatively low Reynolds number and, therefore, a further investigation will be required for the application in the case with much higher Reynolds number. It is notable that this imperfectness did not appear in the application of incompressible flow. Therefore, convective boundary condition should be more closely studied in a compressible case where the pressure is linked to the flow field by an equation of state chosen. As stated earlier, Reynolds number estimated with inlet bulk velocity and duct diameter was 23,000 to match that of the experiments and the Prandtl number, Pr, was assumed to unity for simplicity.

The computational grid is shown in Fig. 9. To take advantage of parallel computation using 8 CPUs, the present domain was split into 8 blocks. Message passing through the CPUs can be made using MPI. In each CPU, the computational load was equally distributed to enhance the computation efficiency. A higher density of grid distribution near the pipe surface was for the better resolution of the near-wall region. Since the mixing layer resulting from the interaction of oxidizer flow with the wall blowing was generated away from the wall, a careful distribution of grid was necessary in the radial direction. Approximately 65 grid points were used in the azimuthal direction and this grid system gave a reasonably acceptable 1st and 2nd order statistics.

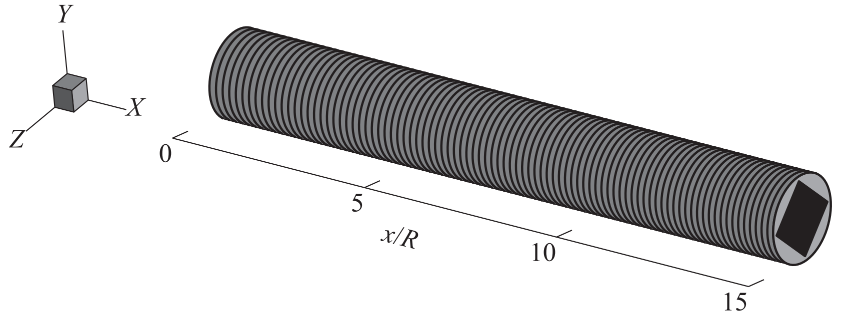

Figure 9 Grid distribution in the present numerical domain

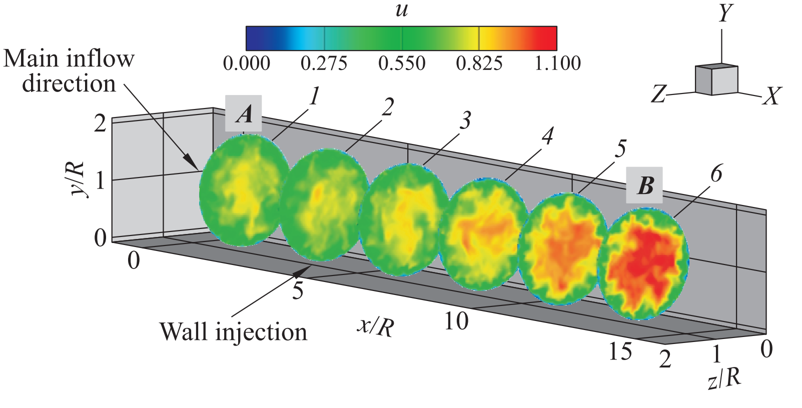

Figure 10 Evolution of streamwise velocity component in the main flow direction: *1* — $x/R = 1.65$; *2* — 4.05; *3* — 6.45; *4* — 8.85; *5* — 11.25; and *6* — $x/R = 13.75$.

Streamwise velocity contours at several streamwise locations are shown in Fig. 10. The stations A and B of the figure indicate the locations of $x/R = 1.65$ and $x/R = 13.75$, respectively. Thus, the station A is located in the simple pipe region without wall blowing and the station B is located in the region of main interest with wall blowing. It clearly shows that the velocity distribution could change due to the wall blowing.

A comparison with the experimental observation is made in Fig. 11. In the experimental data, it is shown that relatively lighter area is developed in the near-wall region due to the presence of combustion flame. The contour pattern of the streamwise velocity resulting from the combustion process resembles the contours found in the data of $x/R = 13.75$. The contour boundary of red region

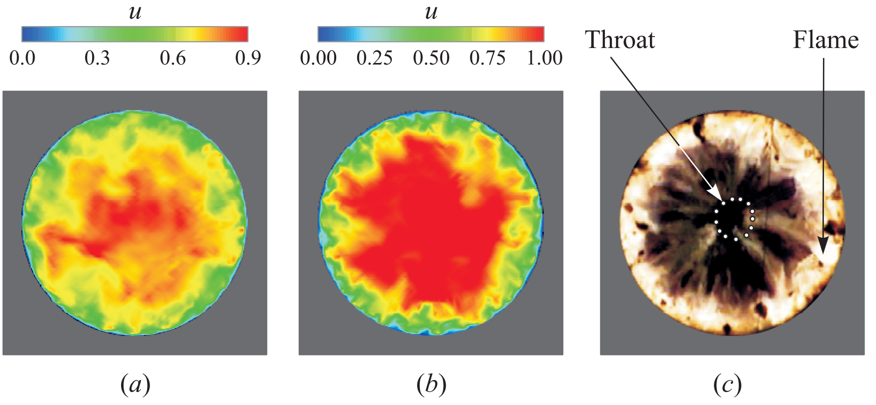

Figure 11 Comparison of streamwise velocity profiles with the visualized photo [12]: (a) A: $x/R = 1.65$; (b) B: $x/R = 13.75$; and (c) experiment.

corresponds approximately to the axial velocity of $u = 0.75$. This comparison qualitatively implies that combustion may take place only in the near-wall region with the axial velocity less than 0.75. Also, it appears that even without actual combustion process in the flow simulation, cold flow is able to reasonably represent the actual situation.

As stated eariler, the most peculiar characteristics of the turbulent flow in the presence of wall blowing is the quasi-periodic shedding of the large-scale vortices. It is believed that those structures were born and grew in the mixing layer away from the surface. Direct identification of those structures is very difficult in a turbulent flow regime as contrary to the larminar flow but both pressure and spanwise vorticity showed some indications of vortex shedding. For example, the time history of pressure shown in Fig. 12a suggested the existence of them. Note that the pressure signal in the region without wall blowing did not exhibit any percular time-scale. However, it is clear that relatively large time-scale was observed after the application of wall blowing. Particularly, at the location of $x/R = 13.75$, the pressure history clearly showed an almost constant time-scale (or equivalently constant frequency). Also, it is noted that the root mean square (rms) value of pressure significantly increased as the flow moved downstream.

Identification of large coherent structures was further pursued in the power spectral density of pressure as shown in Fig. 12b. Again, all the data at the given three streamwise locations showed the peak around $\omega^* \sim 8.8$. This clearly indicates that the quasi-steady vortex shedding was produced. These vortices were obviously produced in the shear layer lifted away from the wall where the main oxidizer flow was being mixed with the wall injected flow. This value of

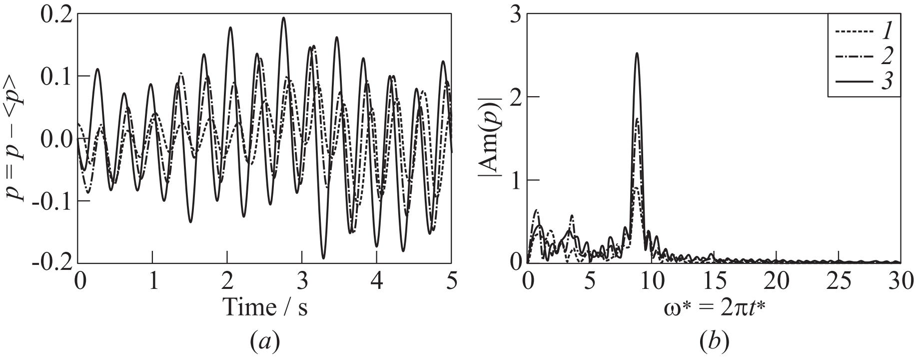

Figure 12 Time history (*a*) and power special density (*b*) of pressure fluctuations at $r/R = 0.001$ at three streamwise locations: *1* — $x/R = 8.75$; *2* — 11.1; and *3* — $x/R = 13.75$

nondimensional parameter known as Strouhal number was also observed in the LES of incompressible flow in a simple channel [2]. Therefore, the surface curvature of the duct and the compressibility appeared not to make any significant change in the qualitative nature of flow features.

One interesting feature of the pressure field is related to the possible distortion of shed vortices. Iso-contour of 3D data of pressure is shown in Fig. 13. In region *I* where the flow develops without wall blowing, there is no directional preference in the pressure fluctuation. However, iso-contours in region *II* where wall blowing was activated, exhibited a distorted surface of pressure field. At the moment, it is not known what causes this distortion but it is conjectured that the distortion of shed vortices is related to this behavior. In the presence of various types of disturbances in turbulent flow, any doughnut-like vortices

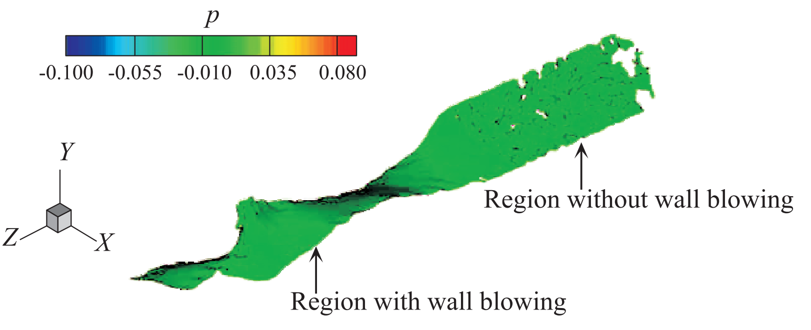

Figure 13 Iso-contour of pressure fluctuation.

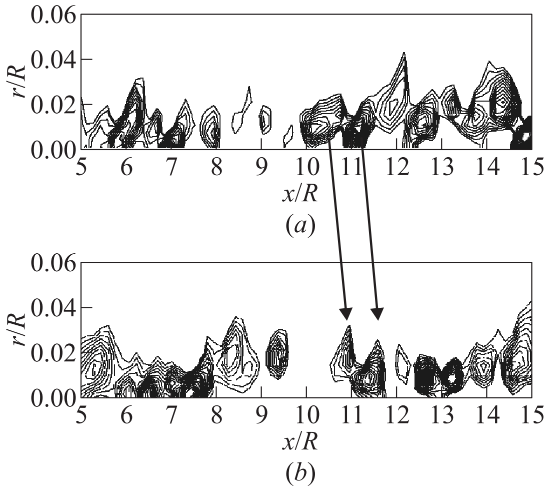

Figure 14 Evolution of azimuthal vorticity (ω_θ) fields in the region with wall blowing

is likely to be susceptible to external agitation and, in turn, this distortion is thought be be reflected in the pressure field as shown in Fig. 13.

Figure 14 shows the evolution of azimuthal component of vorticity profiles in the axial direction in region II with wall blowing detected at two different instants slightly separated apart. This figure shows another evidence for the existence of large-scale vortices. Note that this feature was not found in region I and that the most of vortices were confined in a very thin region near the surface below $r/R < 0.02$. Although the domain of influence of vorticity in the flow gradually expanded toward the center of the duct as the flow moved downstream, vortex centers remained within this shear thin layer developed away from the wall.

4 SUMMARY

Motivated by the fact that the nonlinear combustion in solid rocket motor was frequently caused by the resonance of the shedding vortices with external disturbances near the fuel surface, the present study made an attempt of identifying the role of those large-scale vortices produced in the shear layer near the fuel surface in the hybrid rocket motor. Disturbances include the flow modification caused by different types of disks equipped in prechamber. A PMMA/GOx combination was used for the combustion tests to investigate the unsteady behavior of vortex shedding and subsequent nonlinear combustion process.

Pressure signal only in the case with disk4 showed a sudden pressure drop of about 10 psi during the nominal combustion test. The sudden discontinuity in pressure signal may better be described by a negative DC-shift reported in the literature occasionally observed in solid rocket motor. The mechanism of this type of negative DC-shift is not fully understood and, thus, this phenomenon was not successfully connected to the observed pressure drop in the test with disk4. Possibly, the modified flow or newly induced vortices caused by the disk4 acted to suppress the shedding vortices and, thus, the subsequent combustion process. If this is the case, the phase information of the disturbance produced by the disk4 will be critical and the correlation between this disturbance and shedding vortices generated in the mixing layer by the interaction of the main oxidizer and the gasified stream coming out of the fuel surface should provide a decisive clue.

A LES study was also conducted in a simplified geometry to understand the baseline combustion test. Similar to the result obtained from an incompressible computation without taking into account the wall curvature effect, compressible flow in a duct flow exhibited a peculiar time-scale of $\omega^* \sim 8.8$ in the presence of wall blowing. This finding indicates that the basic flow features with vortex shedding were not significantly modified by either compressibility or curvature effects. Power spectral density or azimuthal component of vorticity conveniently exhibited the presence of dominant frequency. Since the effect of various types of disks tested in the prechamber of the accompanying tests were not investigated in the present numerical study, it was not possible to explain the negative pressure drop observed experimentally. Therefore, the future study will be to implement flow disturbances devices such as various types of disks considered in the experiment. The correlation of phase information between the external disturbance and the vortices characterized by $\omega^* \sim 8.8$ might be able to provide very valuable information for the DC-shift phenomenon.

ACKNOWLEDGMENTS

This work was supported by 2011 research grants of National Research Foundation (2011-0027980) in Korea.

REFERENCES

1. Na, Y., and C. Lee. 2008. Intrinsic flow oscillation in channel flow with wall blowing. AIAA Paper No. 2008-5019.
2. Lee, C., and Y. Na. 2009. Large eddy simulation of flow development in chamber with surface mass injection. *J. Propul. Power* 25(1):51–59.

3. Na, Y., and C. Lee. 2010. Frequency response of turbulent flow to momentum forcing in a channel with wall blowing. *J. Korean Soc. Aeronautical Space Sci.* 1:64–72.
4. Malhotra, S., and G. A. Flandro. 1997. On the origin of the DC shift. AIAA Paper No. 97-3249.
5. Flandro, G. A., J. Majdalani, S. R. Fischbach, and J. C. French. 2004. Nonlinear rocket motor stability prediction: Limit amplitude, triggering and mean pressure shift. AIAA Paper No. 2004-4054.
6. Dijkstra, F. 1990, Ultrasonic regression rate measurement in solid fuel ramjets. AIAA Paper No. 1990-1963.
7. Avres, J. P., and H. S. Jones. 1997. Explanation of DC-shift in hybrid rocket motor. AIAA Paper No. 1997-2938.
8. Avres, J. P., and H. S. Jones. 1997. Elimination of DC-shift in hybrid motors. AIAA Paper No. 1997-2939.
9. Boardmann, T. A., R. L. Carpenter, and S. E. Clafin. 1997. A comparative study of the effect of liquid versus gaseous oxygen injection on combustion stability in 11 inch diameter hybrid motors. AIAA Paper No. 1997-2936.
10. Carmicino, C. 2009. Acoustics, vortex shedding, and low-frequency dynamics interaction in an unstable hybrid rocket. *J. Propul. Power* 25(6):1322–35.
11. Kim, B., Y. Na, and C. Lee. 2010. Non-linear combustion and LES analysis with wall blowing in hybrid rocket. AIAA Paper No. 2010-6956.
12. Masugi, M., T. Ide, S. Yuasa, T. Sakurai, N. Shiraishi, and T. Shimada. 2010. Visualization of flames in combustion chamber of swirling-oxidizer-flow-type hybrid rocket engines. AIAA Paper No. 2010-6546.